



HAL
open science

Dissolution effects on the crystallography and Mg/Ca content of planktonic foraminifera *Globorotalia tumida* (*Rotaliina*) revealed by X-ray diffractometry

J. Nouet, F. Bassinot

► **To cite this version:**

J. Nouet, F. Bassinot. Dissolution effects on the crystallography and Mg/Ca content of planktonic foraminifera *Globorotalia tumida* (*Rotaliina*) revealed by X-ray diffractometry. *Geochemistry, Geophysics, Geosystems*, 2007, 8, pp.q10007. 10.1029/2007GC001647 . hal-00377009

HAL Id: hal-00377009

<https://hal.science/hal-00377009>

Submitted on 9 Oct 2020

HAL is a multi-disciplinary open access archive for the deposit and dissemination of scientific research documents, whether they are published or not. The documents may come from teaching and research institutions in France or abroad, or from public or private research centers.

L'archive ouverte pluridisciplinaire **HAL**, est destinée au dépôt et à la diffusion de documents scientifiques de niveau recherche, publiés ou non, émanant des établissements d'enseignement et de recherche français ou étrangers, des laboratoires publics ou privés.



Dissolution effects on the crystallography and Mg/Ca content of planktonic foraminifera *Globorotalia tumida* (Rotaliina) revealed by X-ray diffractometry

Julius Nouet

Université Paris XI, UMR IDES 8148, F-91405 Orsay, France (julius.nouet@u-psud.fr)

Franck Bassinot

LSCE (CNRS-CEA-UVSQ), Domaine du CNRS, F-91198 Gif-sur-Yvette, France (franck.bassinot@lscce.cnrs-gif.fr)

[1] Several authors suggested that the thinning, with increasing depth of deposition, of calcite X-ray diffractometry (XRD) peaks obtained on planktonic foraminifera tests resulted from the preferential removal of their poorly crystallized parts as dissolution increases. By deconvolving XRD peak (104) from *Globorotalia tumida* (surface sediments, Sierra Leone Rise depth transect), we show that the full width at midheight does not depend only upon crystallinity, but reflects also the chemical and structural heterogeneity of foraminifera tests, which results in closely spaced, individual (104) diffraction peaks corresponding to phases with slightly different Mg contents. *G. tumida* contains two calcite phases: a well crystallized, Mg-poor calcite and a poorly crystallized, Mg-richer calcite. Increasing dissolution results in the preferential removal of the Mg-richer calcite and the improvement of its crystallinity, whereas the Mg-poor calcite does not seem to be affected by dissolution between 2750 m and 4950 m of water depth on Sierra Leone Rise.

Components: 4125 words, 4 figures, 2 tables.

Keywords: dissolution; foraminifera; X-ray diffraction; crystallinity; deconvolution.

Index Terms: 1065 Geochemistry: Major and trace element geochemistry; 0419 Biogeosciences: Biomineralization.

Received 27 March 2007; **Revised** 20 July 2007; **Accepted** 27 July 2007; **Published** 17 October 2007.

Nouet, J., and F. Bassinot (2007), Dissolution effects on the crystallography and Mg/Ca content of planktonic foraminifera *Globorotalia tumida* (Rotaliina) revealed by X-ray diffractometry, *Geochem. Geophys. Geosyst.*, 8, Q10007, doi:10.1029/2007GC001647.

1. Introduction

[2] The substitution of Ca^{2+} by Mg^{2+} during calcite precipitation is thermo-dependent, which gives the opportunity to reconstruct past ocean temperatures by measuring the Mg/Ca ratio of marine calcareous fossils such as foraminifera tests [Nurnberg *et al.*, 1996; Elderfield and Ganssen, 2000]. Post-deposition dissolution at the seafloor leads to the

preferential release of Mg over Ca, as shown by the decrease in Mg/Ca measured on foraminifera tests retrieved from surface sediments along bathymetric transects [Brown and Elderfield, 1996; Rosenthal *et al.*, 2000]. However, we still lack a quantitative dissolution index that would make it possible to accurately correct foraminifera-based, Mg/Ca paleo-thermometer for dissolution overprint. Crystallinity of foraminifera calcite, an estimate of its

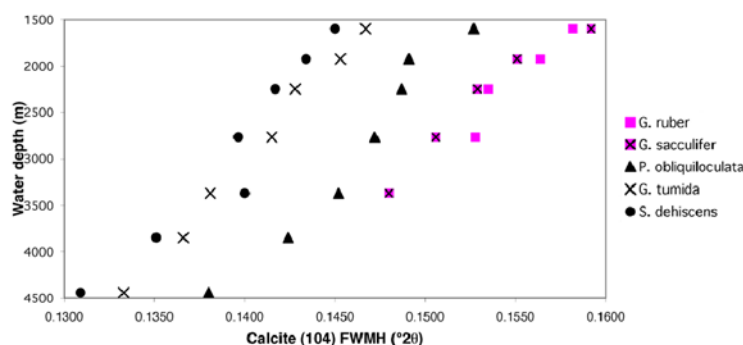


Figure 1. Profiles of water depth versus calcite (104) full width at half maximum (FWMH) of five planktonic foraminifera species picked from surface samples, Ontong Java Plateau, western equatorial Pacific (data from *Bonneau et al.* [1980]).

lattice quality obtained through X-ray diffractometry (XRD), could be a candidate [*Bassinot et al.*, 2004] (Figure 1).

[3] For a “perfect” crystal, of infinite dimensions, X-ray diffraction will occur at the exact angles that meet the Bragg’s criteria $2.d.\sin(\theta) = n.\lambda$ (where θ is the incidence angle, n the diffraction order, λ the X-ray wavelength and d the distance characteristic of a (hkl) plane family). When the crystal is not perfect and is made of small, finite diffracting sub-domains (crystal mosaic), some X-ray diffraction occurs on either side of Bragg’s angles, resulting in the widening of diffraction peaks. The smaller those sub-domains, the broader the X-ray diffraction peaks. The full width at midheight (FWMH) of diffraction peaks is, therefore, an indication of the material crystallinity. A few studies have shown that the crystallinity of calcite that constitutes planktonic foraminifera shells improves as dissolution proceeds (FWMH of XRD peaks diminishes [*Bonneau et al.*, 1980; *Bassinot et al.*, 2004]). These observations suggested that dissolution removes preferentially the poorly crystallized parts of calcite shells. However, as was not pointed out by *Bonneau et al.* [1980] and *Bassinot et al.* [2004], crystallinity might not be the only factor controlling the FWHM of foraminifera calcite XRD peaks. Many foraminifera species used for paleoceanographic reconstructions have a bi-lamellar test or show a surrounding keel, with the result being the presence of at least two types of calcite, which differ slightly in their Mg content [e.g., *Brown and Elderfield*, 1996; *Eggins et al.*, 2003; *Erez*, 2003]. The substitution of Ca^{2+} by Mg^{2+} in calcite reduces the lattice dimensions and results in a shift of X-ray diffraction peaks toward higher angles. For the most energetic diffraction peak (104), a linear relationship between %Mg and angular position (A) can be derived based on

ASTM data (with a Cu X-ray beam) obtained on calcite, dolomite (50% Mg substitution) and magnesite (MgCO_3):

$$[\% \text{Mg substituted}] = 30.966 * A - 910.66 \quad (R2 = 0.99) \quad (1)$$

[4] Thus the width of foraminifera X-ray diffraction peaks may be controlled by calcite crystallinity (size and organization of the diffracting, sub-domains) and/or may result from the stack of several, closely spaced diffraction peaks that correspond to calcite phases with slightly different Mg/Ca ratios. In this paper, we present an analytical and peak deconvolution protocol that we developed to estimate the imprint of those two effects. It has been applied to the study of shells from the planktonic species *Globorotalia tumida* retrieved in surface sediments along a depth transect in the eastern equatorial Atlantic. Our preliminary results make it possible to better understand how dissolution mechanisms affect foraminifera tests and how it may disturb Mg/Ca paleo-thermometer.

2. Diffractometry-X on Powder and Experimental Protocol

[5] Powder is installed on a sample holder, its surface made plane and located tangent to the focalization circle (Rowland circle). When a X-ray beam of known wavelength (λ) hits this powder made of crystallized particles, the (hkl) plans of inter-reticular distance d that respect Bragg’s conditions ($2.d.\sin(\theta) = n.\lambda$, with θ the incidence angle of the X-ray beam on the crystal plans) will result in a positive interference (diffraction) at an angle 2θ . Because foraminifera tests weigh only a few micrograms, we developed a protocol using a “zero-background,” silicium mono-crystal sample



holder that makes it possible to work with small amounts of powder (around 250 μg) and we concentrated on the most energetic diffraction peak of calcite, the peak (104).

[6] Analyses were performed on the Xpert Pro from *Panalytical*, equipped with a Cu X-ray tube and a Ni filter that eliminates the Cu K_{β} X-ray. In order to estimate and reduce the peak widening linked to instrumental effects, settings of the machine were optimized using a well crystallized Iseland spar powder as a control standard. Best results were obtained using 0.02 rad Sollers slots and a X-ray divergence angle set to 0.25° rad. Diffraction profiles were sampled at a $0.004^{\circ}2\theta$ resolution. With these settings, ten replicates of the same Iseland spar powder resulted in a peak (104) mean angular position of $29.420 \pm 0.001^{\circ}2\theta$ (1σ) and a FWHM of $0.042 \pm 0.004^{\circ}2\theta$ (1σ). Using 250 μg of Spath calcite, the 1° -wide scanning of peak (104) is performed in 25 min and results in $\sim 15,000$ photons counted at the peak maximum, with a signal/noise ratio in the order of 25.

[7] To prepare the powder, calcite material was gently crushed in an agate mortar. In order to correct angular position for possible instrumental drawbacks (ex. goniometer position) and preparation problems (extra-thickness), we added 50% of fine-grained quartz powder to all our samples. The angular position of calcite peak (104) was corrected, if necessary, through linear regression using the bracketing quartz (101) and (112) peaks. The powder was evenly distributed upon the zero-background sample holder within a drop of ethanol. The use of alcohol makes it possible to smear the powder more efficiently and avoid extra-thickness that would result in angular shifts of the diffracted peaks. Each sample was run at least three times and the final result was calculated as the average of separate runs. Sample preparation and instrumental limitations result in an overall uncertainty of $\pm 0.005^{\circ}2\theta$ (1σ) for FWHM measurements.

3. Deconvolution Procedure

[8] In order to separate the possible contributions of calcites with different Mg/Ca, we deconvolved the (104) diffraction peaks of foraminifera tests using the *Profile Fit* software. The relative contribution of $K_{\alpha 1}$ and $K_{\alpha 2}$ to the total Cu X-ray is known and was easily taken into account during the deconvolution procedure using two repartition functions (pseudo-Voigt) with an intensity ratio 1/2. Peak broadening due to the presence of several

calcite phases with different Mg contents is likely to be non-symmetrical as Mg-rich layers in foraminifera tests appears to represent a smaller contribution relative to the Mg-poor layers [e.g., *Brown and Elderfield*, 1996; *Benway et al.*, 2003; *Eggins et al.*, 2003; *Erez*, 2003]. Despite the optimization of our analytical protocol, however, some amount of peak asymmetry still results from instrumental and preparation drawbacks. In order to take this analytical asymmetry into account, we forced the shape of deconvolved calcite (104) peaks to match the (104) peak shape obtained from a *Prolabo* pure calcite precipitate powder that is likely to correspond to a mono-phased calcite. This shape forcing was done in *Profile Fit* by setting the asymmetry factor A to 10, and shape factors μ and ε to 0.5. Those factors determine the shape of deconvolved peaks but have no effect on their FWHM. With these pre-set values, the *Profile Fit* software determines the position and relative intensity of the contributing, individual peaks, which are manually incremented until their addition reproduces the initial X-ray peak envelope with a residual error lower than 1%. Thus, each individual peak obtained through deconvolution of the total (104) XRD envelop of a multiphased calcite sample will correspond to a unique calcite phase whose peak geometry is forced, but whose FWHM is dependent on its crystallinity and whose angular position is dependent on Mg/Ca content.

[9] To test our approach, we have analyzed a red coral (*Corallium rubrum*), which presents two calcite structures: a massive, internal trunk surrounded by a porous envelop made of small calcite spicules (Figure 2). When measuring the powder obtained by crushing a sub-sample containing both the trunk and the envelop, the deconvolution procedure successfully separated two calcite phases. The more abundant phase, with a (104) peak centered at $29.71^{\circ}2\theta$ ($\sim 9\%$ Mg substituted to Ca, estimated using equation (1)) is poorer in Mg and better crystallized (FWHM = $0,100^{\circ}2\theta$) than the minor phase, which shows a (104) peak at $29.78^{\circ}2\theta$ ($\sim 11\%$ Mg) and a FWHM = $0,167^{\circ}2\theta$. The Mg/Ca ratios have been independently checked by analyzing Mg/Ca of the trunk and the envelop on an ICP-AES (Inductively Coupled Plasma-Atomic Energy Spectroscopy) using the standard cleaning and measurement approach used for foraminifera-based Mg/Ca thermometry [*de Villiers et al.*, 2002; *Barker et al.*, 2003]. Resulting Mg/Ca values obtained for the trunk and envelop are 11% and 13%, respectively. These results confirm that the envelop is $\sim 2\%$ richer in

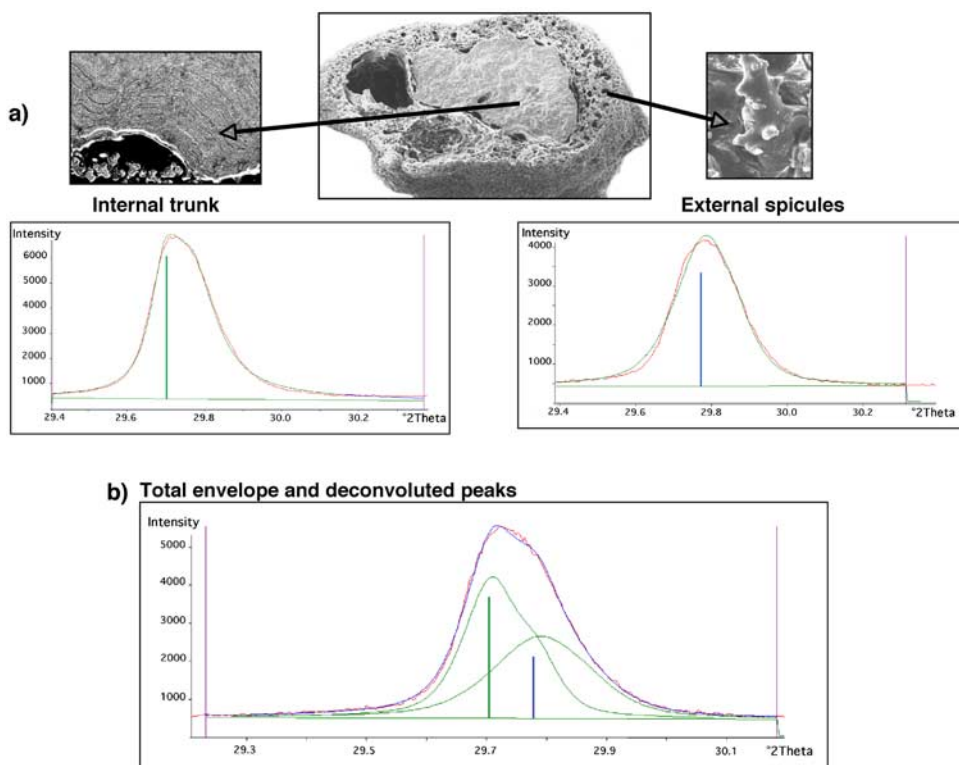


Figure 2. (a) Calcite (104) peaks obtained by analyzing separately the inner (trunk) and outer (spicules) parts of a sample of *Corallium rubrum*. (b) Total calcite (104) envelope obtained by analyzing *C. rubrum* as a whole, plotted with the two constitutive peaks obtained through deconvolution.

Mg than the trunk. It is interesting to note, however, that ICP-AES values are consistently higher than those derived from XRD data. Such an excess %Mg measured in ICP-AES relative to XRD data has already been observed for other marine biogenic calcites (unpublished results), with excess %Mg reaching up to ~4%. We interpret these results as an indication that part of the Mg content measured by ICP-AES is actually located outside the crystal lattice (possibly associated to organic compounds), and not substituted to Ca in the calcite.

[10] When performing XRD analyses separately on the trunk and the envelop (mechanical separation before crushing), the FWMH measured on the two

calcite differed by up to $0.02^\circ 2\theta$ compared to the deconvoluted values obtained from the whole sample (Table 1). Such a rather large difference prompted us to look carefully at uncertainties that might be associated to angular positions and FWMH estimated obtained through the deconvolution of the (104) peak from foraminifera tests. Because the separation of foraminifera layers cannot be performed mechanically, we estimated those deconvolution uncertainties by running through *Profile Fit* a set of synthetic diffraction peaks, each obtained by merging diffraction peaks of known angular position and FWMH. By comparing deconvoluted values to initial (known) values it was possible to infer the accuracy of the

Table 1. Data Resulting From the Deconvolution of *Corallium rubrum*

	Trunk Alone	Spicules Alone	Total Sample	
			Phase 1 Deconvoluted	Phase 2 Deconvoluted
Angular position, $^\circ 2\theta$	29.703	29.773	29.705	29.777
FWMH, $^\circ 2\theta$	0.121	0.168	0.100	0.167
Surfaces ratios, %	≈75	≈25	55	45
Mg/Ca molar ratios (ICP-AES)	11.3%	13.1%		

Table 2. Sample Locations With the Mg Contents and Lattice Parameters of the Two Calcite Phases Obtained by Deconvolving the Calcite (104) XRD Peak From *G. tumida* Shells, Along a Bathymetric Profile of Sierra Leone Rise

	Water Depth, m	Localization (Lat., Long.)	Total Signal		Deconvoluted Signal				
			FWMH, $^{\circ}2\theta$	Angular Position, $^{\circ}2\theta$	Phase	Angular Position, $^{\circ}2\theta$	FWMH, $^{\circ}2\theta$	Angular Variation, $^{\circ}2\theta$	Surfaces Ratio, %
Station A	2750	5°07N 21°01W	0.060	29.430	Peak 1	29.431	0.055	0.014	39.35
Station B	3200	5°25N 21°31W	0.059	29.429	Peak 2	29.445	0.220	0.013	38.36
					Peak 1	29.430	0.053		
Station C	3560	5°32N 21°48W	0.055	29.428	Peak 2	29.443	0.212	0.012	32.96
					Peak 1	29.429	0.052		
Station D	3890	5°50N 22°48W	0.060	29.432	Peak 2	29.441	0.199	0.013	36.78
					Peak 1	29.432	0.056		
Station E	4250	7°00N 24°37W	0.058	29.429	Peak 2	29.447	0.212	0.012	35.76
					Peak 1	29.430	0.054		
Station F	4750	7°43N 24°37W	0.056	29.426	Peak 2	29.443	0.20	0.011	35.1
					Peak 1	29.426	0.052		
Station G	4950	8°57N 24°29W	0.055	29.427	Peak 2	29.437	0.191	0.008	32.53
					Peak 1	29.427	0.051		
					Peak 2	29.435	0.190		

deconvolution procedure. The range of Mg/Ca variability within the shell of a single planktonic foraminifera is less than 10 mmol/mol [Brown and Elderfield, 1996; Eggins et al., 2003], which corresponds to a maximum (104) peak angular shift $\leq 0.01^{\circ}2\theta$ (estimated from equation (1)). Within this small range, our tests indicate that the uncertainty on the deconvolved angular position is $\pm 0.01^{\circ}2\theta$, but the uncertainty is only $\pm 0.005^{\circ}2\theta$ on the estimate of FWMH. Thus the deconvolution of (104) diffraction peaks obtained on foraminifera tests will provide better estimates of FWMH than of angular shifts related to differences in Mg content.

4. Application to Planktonic Foraminifera *G. tumida*

[11] To analyze the effects of dissolution on crystallinity and Mg/Ca ratios of planktonic foraminifera

tests, we have worked on *Globorotalia tumida* retrieved in surface sediments from a depth transect in the Sierra Leone Rise (equatorial Atlantic; Table 2). Previous studies performed using total sediment crystallinity and planktonic species *Globigerinoides ruber* shell weight had clearly shown that, as expected, carbonate dissolution increases with water depth along this transect and has a clear effect on biogenic calcite preservation [Gehlen et al., 2005]. The *G. tumida* species was chosen for this study because it is known to be dissolution-resistant, which makes it available across a wide range of bottom water saturation relative to calcite (it was abundant all along the transect, from 2750 to 4950 m of water depth). Furthermore, because its test is large and relatively heavy, picking 30–40 specimens per sample provided enough material for accurate XRD analyses ($\geq 600 \mu\text{g}$ which resulted in peak (104) intensity always above 8,000 photon counts).

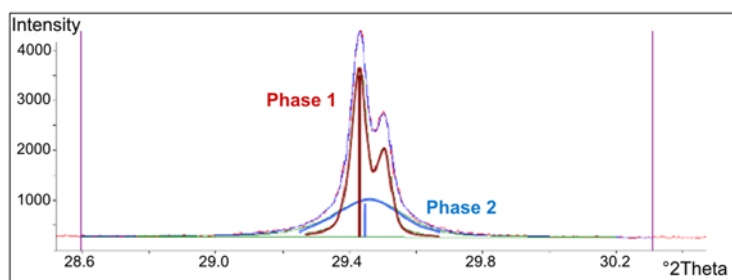


Figure 3. An example of peak (104) obtained from *Globorotalia tumida* X-ray diffraction plotted with its corresponding deconvolved phases.

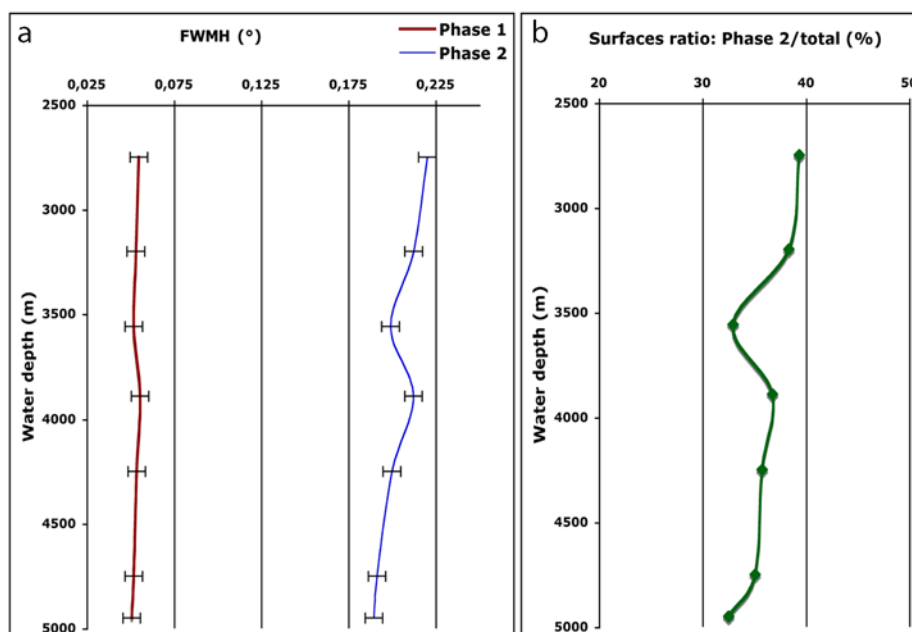


Figure 4. (a) Profiles of water depth versus the full width at half maximum (FWMH) of the two phases deconvolved from *G. tumida* diffraction peak (104). Phase 1 (lower in Mg) is better crystallized (smaller FWHM value) and does not show a change in FWHM with increasing depth of deposition, whereas phase 2 (richer in Mg) is poorly crystallized (larger FWHM value) and shows a clear trend of decreasing FWHM (increasing crystallinity) along the depth transect. (b) Profile of water depth versus the relative proportion of calcite phase 2 (richer in Mg) obtained by deconvolving *G. tumida* diffraction peak (104). The proportion of phase 2 decreases with increasing depth of deposition, indicating a preferential loss of the Mg-richer phase in the *G. tumida* tests as dissolution increases.

[12] Our results show that FWHM measured on the total envelop of XRD peak (104) decreases along the depth transect, from $0.060^{\circ}2\theta$ at 2750 m of water depth to $0.054^{\circ}2\theta$ at 4950 m (Table 2). This decrease is coherent with previous observations made by *Bonneau et al.* [1980] and *Bassinot et al.* [2004], although it remains small with respect to the precision of the measurement ($\pm 0.005^{\circ}2\theta$).

[13] The deconvolution of (104) peaks shows the presence of two calcite phases in *G. tumida* at each station (Figure 3). The average angular positions of these two calcitic phases are $29.429 \pm 0.003^{\circ}2\theta$ and $29.440 \pm 0.007^{\circ}2\theta$, respectively (Table 2). This angular difference suggests that the second phase is slightly richer in Mg. Their respective intensities (estimated from deconvolved peak surfaces) indicate that the Mg-poor phase represents about 70% of the total calcite. The relative proportion of the Mg-rich phase decreases slightly with increasing depth of deposition, varying from 39% at 2750 m to 33% at 4950 m (Figure 4b).

[14] The Mg-poor phase (phase 1) shows a narrow XRD (104) peak (average FWHM = $0.053^{\circ}2\theta$ along the transect). This FWHM does not vary

noticeably with water depth and stays within the error bar ($0.005^{\circ}2\theta$, Figure 4a). The Mg-rich phase (phase 2), on the other hand, shows a wider XRD (104) peak (average FWHM = $0.203^{\circ}2\theta$ along the transect), which gets finer with increasing water depth of deposition (FWHM varies from $0.220 \pm 0.005^{\circ}2\theta$ at 2750 m to $0.189 \pm 0.005^{\circ}2\theta$ at 4950 m; Figure 4a).

5. Discussion and Conclusion

[15] *G. tumida* is a planktonic species that develops a characteristic keel. The presence of two calcite phases with slightly different Mg contents and crystallinity seems to be coherent with previous studies of the Mg distribution within *G. tumida* tests [*Brown and Elderfield*, 1996]. By performing electron microprobe measurements on *G. tumida*, these authors clearly identified two calcite phases: a Mg-rich, “inner” calcite referring to the inside of the chambers (average Mg/Ca of 5.1 mmol/mol) and a Mg-poor, “outer” calcite (average Mg/Ca of 2.1 mmol/mol) that corresponds to the external crust, mainly composed of the keel. They estimated the relative amount of these two calcites to be 30–



70% (the same respective proportions that we found from XRD results) and observed a preferential loss of the Mg richer calcite with increasing depth of deposition. These independent microprobe results indicate that the deconvolution of XRD calcite peaks makes it possible to see the respective evolution of the outer (keel) and inner (chambers) calcites of *G. tumida* during dissolution along the Sierra Leone Rise depth transect.

[16] As far as dissolution mechanisms are concerned, our data show that the Mg-poor calcite does not seem to be noticeably affected, and that the progressive dissolution of *G. tumida* tests along the depth transect is marked mostly by (1) the preferential removal of the Mg-richer calcite (Figure 4b) and (2) an increase in the crystallinity of this calcite (decrease in FWMH; Figure 4a). A few data, however, do not follow the general trends with water depth. At station C, both the FWMH and the relative proportion of Mg-rich calcite (phase 2) are noticeably lower than expected from the rest of the transect, suggesting an enhanced dissolution at that depth (Figures 4a and 4b). This may indicate that dissolution intensity is not only related to water depth and that local factors may play a role (e.g. spatial variations in respiration-driven dissolution). At station D, the Mg-richer calcite shows an anomalously high FWMH ($0.212^\circ 2\theta$). Such a value could be expected if downslope sedimentary movements had recently brought well-preserved material from a shallower depth. However, this hypothesis is ruled out by the fact that the relative proportion of the Mg-rich calcite (also dissolution-sensitive) at station D is coherent with the rest of the transect (Figure 4b). At present, there is no clear explanation for the anomalously high FWMH of station D and further data will be needed to solve this problem.

[17] By looking at the FWMH evolution of the total (104) calcite peak with increasing dissolution, *Bonneau et al.* [1980] and *Bassinot et al.* [2004] had already suggested that dissolution might remove preferentially the poorly crystallized part of planktonic foraminifera tests. Our new data make it possible to go a step further, as they indicate that it is the poorly crystallized parts of the Mg-rich phase that are first affected by dissolution, thus explaining the overall increase in crystallinity of foraminifera tests and also the decrease of Mg/Ca that has been observed by many authors [e.g., *Nurnberg et al.*, 1996; *Elderfield and Ganssen*, 2000]. The fact that only the poorly crystallized, Mg-rich calcite suffers from dissolu-

tion is true, at least, for early stages of dissolution that we could address on this Atlantic depth transect. Future work on Pacific depth transects, where bottom water undersaturation with respect to calcite is more extreme than at Sierra Leone Rise, will make it possible to look at the more advanced stages of dissolution, where calcite that constitutes the chambers is more severely affected, which should even lead to highly dissolved samples where the keel only is preserved.

[18] The use of calcite crystallinity might be of interest as a dissolution proxy, in general, but more particularly for Mg/Ca paleothermometry. If future works show that the initial (non-dissolved), relative proportion of Mg-rich versus Mg-poor calcite(s) is rather constant for a given foraminifera species or is variable but controlled by known environmental factors, then the proportion of these different calcite phases measured from XRD analyses on shells picked from deep-sea sediments might make it possible (1) to address how much of the initial structure has been modified through dissolution and (2) to correct paleothermometry Mg/Ca data for the relative loss of the Mg-richer calcites.

Acknowledgments

[19] Special thanks go to P. Pradel for his invaluable technical assistance and friendly support throughout this research project. F.B. thanks Marion Gehlen and D. McCorkle for providing the Sierra Leone Rise samples retrieved during cruise KN159 of the R/V *Knorr* and F. Mélières for providing the Iseland spar sample and for fruitful discussions on calcite crystallography. J.N. thanks J. P. Cuif and Y. Dauphin for providing the red coral sample. This research project was supported through an ANR/FORCLIM contract and through a contribution from the LSCE (CNRS-CEA-UVSQ, LSCE contribution 2810).

References

- Barker, S., M. Greaves, and H. Elderfield (2003), A study of cleaning procedures used for foraminiferal Mg/Ca paleothermometry, *Geochem. Geophys. Geosyst.*, 4(9), 8407, doi:10.1029/2003GC000559.
- Bassinot, F. C., F. Mélières, M. Gehlen, C. Levi, and L. Labeyrie (2004), Crystallinity of foraminifera shells: A proxy to reconstruct past bottom water CO₃ changes?, *Geochem. Geophys. Geosyst.*, 5, Q08D10, doi:10.1029/2003GC000668.
- Benway, H. M., B. A. Haley, G. P. Klinkhammer, and A. C. Mix (2003), Adaptation of a flow-through leaching procedure for Mg/Ca paleothermometry, *Geochem. Geophys. Geosyst.*, 4(2), 8403, doi:10.1029/2002GC000312.
- Bonneau, M. C., F. Mélières, and C. Vergnaud-Grazzini (1980), Variations isotopiques (oxygène et carbone) et cristallographiques chez des espèces actuelles de foraminifères planctoniques en fonction de la profondeur de dépôt, *Bull. Soc. Geol. Fr.*, 22(5), 791–793.



- Brown, S. J., and H. Elderfield (1996), Variation in Mg/Ca and Sr/Ca ratios of planktonic foraminifera caused by post depositional dissolution: Evidence of shallow Mg-dependent dissolution, *Paleoceanography*, *11*(5), 543–552.
- de Villiers, S., M. Greaves, and H. Elderfield (2002), An intensity ratio calibration method for the accurate determination of Mg/Ca and Sr/Ca of marine carbonates by ICP-AES, *Geochem. Geophys. Geosyst.*, *3*(1), 1001, doi:10.1029/2001GC000169.
- Eggins, S., P. De Deckker, and J. Marshall (2003), Mg/Ca variation in planktonic foraminifera tests: Implications for reconstructing palaeo-seawater temperature and habitat migration, *Earth Planet. Sci. Lett.*, *212*, 291–306.
- Elderfield, H., and G. Ganssen (2000), Past temperature and delta ¹⁸O of surface ocean waters inferred from foraminiferal Mg/Ca ratios, *Nature*, *405*, 442–445.
- Erez, J. (2003), The source of ions for biomineralization in foraminifera and their implications for paleoceanographic studies, in *Biomineralization, Rev. Mineral. Geochem.*, vol. 54, edited by P. M. Dove, J. J. de Yoreo, and S. Weiner, pp. 115–149, Mineral. Soc. of Am., Washington, D. C.
- Gehlen, M., F. C. Bassinot, L. Chou, and D. McCorkle (2005), Reassessing the dissolution of marine carbonates: I. Solubility, *Deep Sea Res., Part I*, *52*, 1445–1460.
- Nurnberg, D., J. Bijma, and C. Hemleben (1996), Assessing the reliability of magnesium in foraminiferal calcite as a proxy for water mass temperatures, *Geochim. Cosmochim. Acta*, *60*(5), 803–814.
- Rosenthal, Y., G. P. Lohmann, K. C. Lohmann, and R. M. Sherrell (2000), Incorporation and preservation of Mg in Globigerinoides sacculifer: Implications for reconstructing the temperature and ¹⁸O/¹⁶O of sea water, *Paleoceanography*, *15*(1), 135–146.